Microchim Acta (2017) 184:707–713
DOI 10.1007/s00604-016-2059-1

ORIGINAL PAPER

Rattle-type Fe_3O_4@SnO_2 core-shell nanoparticles for dispersive solid-phase extraction of mercury ions

Ali Mehdinia[1] · **Mina Jebeliyan**[2] · **Tohid Baradaran Kayyal**[2] · **Ali Jabbari**[2]

Received: 29 July 2016 / Accepted: 11 December 2016 / Published online: 20 December 2016

Abstract The synthesis of rattle-type nanostructured Fe_3O_4@SnO_2 is described along with their application to dispersive solid-phase extraction of trace amounts of mercury(II) ions prior to their determination by continuous-flow cold vapor atomic absorption spectrometry. The voids present in rattle-type structures make the material an effective substrate for adsorption of Hg(II), and also warrant high loading capacity. The unique morphology, large specific surface, magnetism property and the synergistic effect of magnetic cores and SnO_2 shells render these magnetic nanorattles an attractive candidate for solid-phase extraction of heavy metal ions.The sorbent was characterized by transmission electron microscopy, scanning electron microscopy, FTIR, energy-dispersive X-ray spectroscopy and by the Brunnauer-Emmett-Teller technique. The effects of pH value, adsorption time, amount of sorbent, volume of sample solutions, concentration and volume of eluent on extraction efficiencies were evaluated. The calibration plot is linear in the 0.1 to 40 μg·L^{-1} concentration range, and the preconcentration factor is 49. The detection limit is 28 ng·L^{-1}. The sorbent was applied to the analysis of (spiked) river and sea water samples. Recoveries ranged from 97.2 to 100.5%.

Electronic supplementary material The online version of this article (doi:10.1007/s00604-016-2059-1) contains supplementary material, which is available to authorized users.

✉ Ali Mehdinia
mehdinia@inio.ac.ir

[1] Department of Marine Living Science, Ocean Science Research Center, Iranian National Institute for Oceanography and Atmospheric science, Tehran 14118-13389, Iran

[2] Department of Chemistry, Faculty of Science, K. N. Toosi University of Technology, Tehran 15418-49611, Iran

Keywords Rattle-type structure · Yolk-Shell · Tin oxide · Nanostructure · Dispersive solid-phase extraction · Mercury ions · Water analysis · Transmission electron microscopy · Scanning electron microscopy

Introduction

Over the past decade, dispersive magnetic solid phase extraction (MSPE) has attracted widespread attractions in separation science [1]. In this regard, magnetic nano-adsorbents provided excellent practicable performance because of their magnetic susceptibility, high effectual specific surface area and high capability to functionalize the surface [2]. The unique magnetic property enables a facile separation of nano-adsorbents by applying an external magnetic field. However, owing to contamination, agglomeration and oxidation of the bare magnetic extractants, the adsorption performance of the sorbent can be decreased [1]. Therefore, the development and design of more efficient magnetic sorbents with enhanced adsorption ability is still required.

Magnetic core-shell nanocomposites have been subjected to the wide-ranging studies for the combined functionalities of cores and shells [3]. They exhibit the great potential for utilizing as an MSPE sorbent. For example, the combination of magnetic cores and dielectric metal oxides (e.g. TiO_2 or SnO_2) as shell can provide wonderful opportunity for using the properties of both the magnetic and dielectric materials [3]. Recently, hollow nanostructures with moveable cores, so-called yolk-shell or rattle-type nanocomposites (NCs) have aroused notable interest because of the tailorability and functionality in both the cores and hollow shells [4]. The yolk-shell or rattle-type structure is a special class of core–shell stracture with distinguished core@void@shell configuration [5, 6]. The formed void in yolk-shell structures can provide unique

properties like low density, high specific surface area, potential interior core, designable interstitial void, and more capable outer shell [6]. The simultaneous use of the moveable core, shell, and the interstitial void between the core and the shell in adsorption can cause more exposure of the active sites to the compounds, which in turn prepare much more effectual interaction with the guest molecules [7].

In yolk-shell structures, the outer shell has beneficial roles. Several studies have reported that the outer shell can prevent the aggregation and sintering of the neighboring particles even under harsh reaction situations [7, 8]. The shell can act as a mediator with external environment via the presence of pores, and transportation into and out of the nanorattles can also be possible [8]. According to the structure, a wide range of applications are developed in nanoreactors [9], drug/gene delivery [10], lithium-ion batteries [11], sensors [12], surface enhanced Raman scattering [13], catalysis [14], microwave absorption [3], biomedical fields [15], and so forth.

Numerous approaches have been proposed for the preparation of yolk-shell NCs, which the common synthesis approaches can be divided into three categories consist of hard-template method, soft template method, and template-free synthesis [16]. According to the salient features of the yolk-shell structure, it can be introduced as an appropriate sorbent for solid-phase extraction. The design of magnetic yolk-shell NCs in MSPE procedure was previously performed for detection of trace amount of polycyclic aromatic hydrocarbons through synthesis of a rattle-type microsphere with magnetic-carbon double-layered shells [1]. Recently, Fe_3O_4@$Zr(OH)_x$ yolk-shell nanospheres were examined as adsorbents for the removal of Pb(II) [17]. Therefore, an increasing trend in preparation of SPE sorbent with yolk-shell structures can be expected.

Nano-scale metal oxide materials are one of the most important classes of materials because of their superlative properties and extensive applications in science and technology [18]. A variety of metal oxides (e.g., TiO_2 [19], Al_2O_3 [20]) have been investigated as potential adsorbent for solid phase extraction of heavy metals. Their nanometer size provide a large surface area, a high surface-to-bulk ratio, and surface functional groups that can interact with heavy metal ions [21]. Between various metal oxide nanostructures, SnO_2 is one of the smart materials due to its several interesting properties such as wide band gap (E_g = 3.6 eV, at 300 K), high capacity, surface hydroxyl groups, large surface area, vast temperature stability, high chemical stability and environmental benignity [18, 21].

So far, no study has been reported the use of SnO_2 nanostructures as an adsorbent of solid phase extraction. According to the mentioned properties, SnO_2 nanoparticles can be very promising materials for solid phase extraction procedure.

Mercury is considered to be a perilous environmental pollutant that can lead to various diseases in the brain, kidney, and central nervous system [22]. It can accumulate in biological tissues and impact the entire food chain [23]. Mercury can enter the aquatic system and even in trace amounts can cause health hazards to the human beings and all other microorganisms [24]. Hence, determination of mercury in ultra-trace amounts is extremely important. Herein, we present a simple, flexible and controlled method for the synthesis of yolk-shell nanostructure with magnetic core and SnO_2 shell. Now, attention is being paid to developing simple and efficient methods for fabricating. The synthesis of rattle-type SnO_2 is performed at low temperature. For the etching process, NaOH solution was utilized and autoclave and high temperature was not applied. Importantly, the method requires no prior surface modification, no complicated synthetic processes, corrosive etching agents and high-temperature. In the present study, Fe_3O_4@SnO_2 yolk-shell as a MSPE sorbent was successfully synthesized by an efficient and facile strategy. The yolk-shell was applied for fast and effective extraction of mercury ions from water samples.

Experimental

Materials

Ferric chloride hexahydrate ($FeCl_3.6H_2O$), ferric chloride tetrahydrate ($FeCl_2.4H_2O$), ammonium hydroxide, urea, tetraethyl orthosilicate (TEOS), ethanol, sodium hydroxide, sodium borohydride, mercury(II) chloride were all purchased from Merck (Darmstadt, Germany, www.merckmillipore.com). HCl (37%) was obtained from Scharlau (Barcelona, Spain, www.scharlab.com). Tin (IV) chloride pentahydrate ($SnCl_4.5H_2O$) was also purchased from Sigma-Aldrich (Beijing, China, www.sigmaaldrich.com). All chemicals were analytical grade and used without further purification and deionized (DI) water was also used in all experiments.

Apparatus

All mercury measurements were carried out with an atomic absorption spectrometry (AAS, GBC932 AA, Victoria, Australia) equipped with a vapor generation system (Hydride Generator, GBCHG 3000) with argon (99.99%) as the carrier. Sodium borohydride was utilized as the reducing agent for the determination of Hg^{2+}. The fresh solution was made by addition of 0.3% $NaBH_4$ in 0.5% NaOH. The hydrochloric acid solution (3 mol L^{-1}) was also prepared by dilution of the concentrated HCl. The characterization of rattle-type Fe_3O_4@SnO_2 structures was also carried out by transmission electron microscopy (TEM, LEO 912AB), scanning electron microscopy (SEM, KYKY - EM3200–26 kV), Fourier transform infrared spectroscopy (FT-IR, Bruker, VERTEX 70),

Brunauer-Emmett-Teller (BET, Belcat-a bell Japan inc.) and energy-dispersive X-ray (EDX, Sirius SD, England) analyzes.

Synthesis of adsorbent

Preparation of Fe_3O_4 nanoparticles

The Fe_3O_4 nanoparticles were prepared by a chemical co-precipitation method. The preparation of Fe_3O_4 nanoparticles were carried out by mixing $FeCl_3.6H_2O$ (9.4 g) and $FeCl_2.4H_2O$ (3.5 g) with 160 mL double-distilled water. The solution was stirred under the nitrogen gas atmosphere to prevent possible oxidation. Then, 20 mL of ammonium hydroxide (25% *v*/v) was added drop wise to the solution while increasing the temperature up to 80 °C. The reaction was kept at the mentioned temperature for 30 min. Finally, the black precipitate were rinsed with double-distilled water by magnetic decantation for several times and dried at 50 °C for 4 h [25].

Synthesis of Fe_3O_4@SiO_2 core-shell

The Fe_3O_4@SiO_2 nanoparticles were synthesized through a modified Stöber method. Briefly, Fe_3O_4 particles (0.9 g) were dispersed in a mixture of ethanol (225 mL) and double-distilled water (75 mL) by sonication for 15 min. Subsequently, ammonium hydroxide (15 mL) and TEOS (2.1 mL) were added to the reaction mixture. The resulting solution was held at 40 °C for 12 h under continuous mechanical stirring. The final resulted nanoparticles were separated by magnetic decantation, and washed with ethanol and water, respectively [25].

Synthesis of Fe_3O_4@SnO_2 yolk-shell

0.06 g of the Fe_3O_4@SiO_2 was dispersed in 60 mL of ethanol/water (37.5 vol.% ethanol) solution by sonication for 20 min, followed by addition of urea (0.36 g) and $SnCl_4.5H_2O$ (0.287 g) under stirring [3]. After stirring for 10 min, the mixed solution was heated at 50 °C under stirring for 12 h. The product was rinsed with deionized water four times and dried at 60 °C for 4 h. Then, nanoparticles were dispersed in 100 mL NaOH solution (1 M) and heated at 60 °C for 12 h under stirring. In this regard, NaOH solution was utilized as etching agent of silica layer for the formation of interstitial void in yolk-shell structure. The resulting product was washed with double-distilled water and ethanol by magnetic decantation for four times and dried at 60 °C for 4 h. Figure 1 shows the schematic illustration of synthesis process of Fe_3O_4@SnO_2 yolk-shell nanoarchitecture.

Adsorption and elution characteristics

The removal efficiency is defined as:

$$\text{Removal}\ (\%) = \frac{C_i - C_e}{C_{i.}}$$

Where C_i and $C_e$are attributed to the analyte amount in initial solution and effluent solution after extraction process, respectively.

The relative recovery (RR) for analysis of real water samples are calculated by using Eq.

$$RR = \frac{C_{founded} - C_{real}}{C_{added}}$$

Where $C_{founded}$ is the concentration of analyte in the final solution after spiking of a certain amount of standard solution into the real sample, C_{real} is obtained based on the concentration of analyte in the real sample and C_{added} is also attributed to the concentration of a certain amount of standard which was spiked into the real sample.

MSPE procedure

For MSPE procedure of mercury ions in a batch system, first: 15 mg of Fe_3O_4@SnO_2 nanoparticles were dispersed into 100 mL of aqueous samples, then the pH was adjusted to 6 and the solution was stirred at 400 rpm for 5 min. The room temperature was applied for all of extraction and determination procedures. All experiments were carried out with three replications. Afterwards, nano-adsorbents were separated from the solution by using an external magnetic field and washed with deionized water. In order to elution of mercury ions from the substrate, 2 mL of HNO_3 (0.5 mol L^{-1})/thiourea (2% *w*/*v*) was used. Finally the eluted solution was separated and mercury concentration measured by using CV-AAS.

Results and discussion

Choice of sorbent

To date, metal oxide nanomaterials have widely been introduced as adsorbents which can exhibit favorable sorption to heavy metals [26]. Among nano metal oxides, SnO_2 can be utilized due to outstanding properties which can provide an appropriate substrate by surface hydroxyl groups, proper surface area and chemical stability [27]. Despite the potential properties, the utilization of SnO_2 nanoparticles as a sorbent for SPE has not been reported. Accordingly, in the present work, a sorbent of SPE has been developed based on SnO_2 nanoparticles.

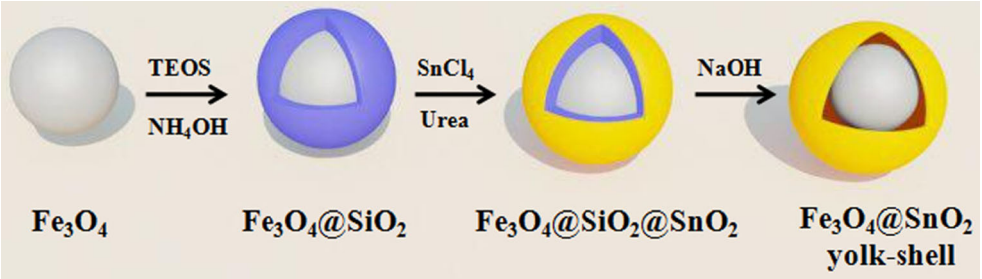

Fig. 1 The schematic illustration of synthesis process of Fe_3O_4@SnO_2 yolk-shell nanoarchitecture

In order to improve the efficiency of SnO_2 substrate, we also applied an effectual configuration via yolk-shell structure with Fe_3O_4 interior core and SnO_2 shell. In this way, the synthesis procedure of yolk-shell Fe_3O_4@SnO_2 nanoparticles is illustrated in Fig. 1. The process includes (1) preparation of Fe_3O_4 by co-precipitation strategy, (2) coating of magnetic nanoparticles with silica layer via sol-gel method, (3) the formation of SnO_2 layer by depositing on silica surface, (4) etching of middle silica layer and the yolk-shell structure. It should be noted that the removal of middle layer can be based on selective etching which lead to the formation of void in hard template method of yolk-shell structure. Furthermore, urea not only play a role to form SnO_2 shell, but also the alkaline condition obtained via the relative hydrolysis of urea can lead to dissolving of silica layer [28]. The resulted composite as a MSPE sorbent was applied for extraction and trace-level determination of mercury ions from aqueous samples.

Characterization of adsorbent

A variety of techniques was utilized for characterization of the rattle-type sorbent (Fig. 2). The FT-IR spectra of the resulted yolk-shell are illustrated in Fig. 2a. The characteristic peak of 548 cm^{-1} is attributed to FeO band. The presence of silanol groups on the surface of Fe_3O_4 was also confirmed by absorptions at 803 cm^{-1} (symmetric vibration of Si-O-Si), 945 cm^{-1} (Si-OH) and 1093 cm^{-1} (asymmetric vibration of Si-O-Si). As shown in Fig. 2a, the peaks located at 640 cm^{-1} and 730 cm^{-1} are likely due to the vibration of Sn − O band in SnO_2 lattice and the absorption peaks at 1627 cm^{-1} and 831 cm^{-1} is assigned to δOH(H_2O) and δOH(Sn–OH), respectively. The attributed peaks to silica coating were eliminated that can approve the presence of the void. Furthermore, the EDX analysis (Fig. 2b) was also used to prove the formation of metal oxides and elimination of silica coating. The amount of silica was determined to be 0% that it can confirm lack of silica layer in the prepared nanoarchitectures. The morphology, size and structure of yolk-shell nanoparticles were evaluated by SEM and TEM analysis. It can be seen in Fig. 2c, that the nanoarchitectures are approximately spherical with an estimated size below 150 nm. In addition, the approximate thickness of SnO_2 shell was obtained in the region of 5 to 15 nm. Based on TEM image, the formation of yolk-shell structure was proved. The BET analysis was also applied for calculating surface area of the sorbent. The surface area of Fe_3O_4@SiO_2 and Fe_3O_4@SnO_2 yolk-shell structure was obtained as 44.9981 m^2 g^{-1} and 105.4841 m^2 g^{-1}, respectively. In this way, increasing surface area is another reason for confirmation of interstitial void formation in the sorbent structure, that it can cause higher loading capacity and extraction efficiency of the target analyte.

Optimization of the extraction procedure

The following parameters were optimized: (a) pH, (b) amount of sorbent, (c), adsorption time, (d) type, concentration and volume of eluent, (e) volume of sample solution on extraction efficiencies. Respective data and Figures are given in the Electronic Supporting Material. We found the following experimental conditions to give best results: (a) A sample pH value of 6; (b) amount of sorbent of 15 mg; (c) adsorption time

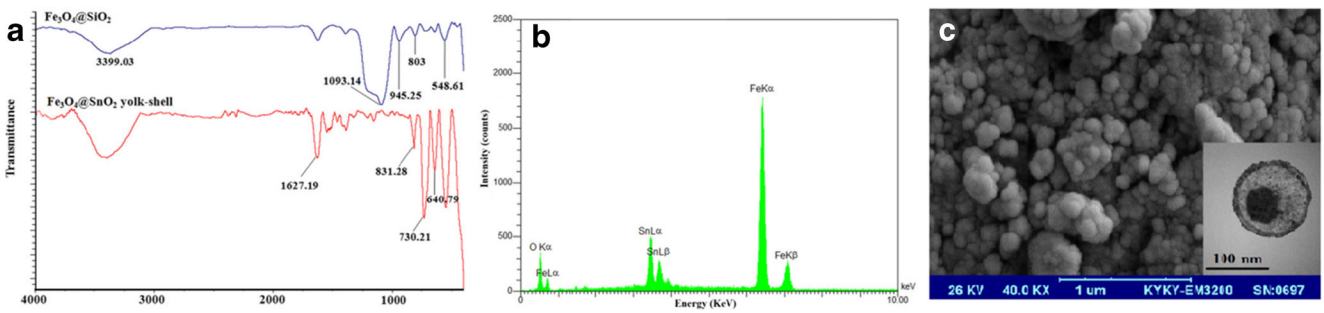

Fig. 2 FT-IR spectra of Fe_3O_4@SiO_2 and Fe_3O_4@SnO_2 yolk-shell (**a**), EDX spectrum (**b**), SEM and TEM images of Fe_3O_4@SnO_2 yolk-shell (**c**)

Table 1 Recovery of Hg^{2+} in the presence of possible interfering species in aqueous solution

Interfering ion	Concentration (μg L^{-1})	Recovery (%)
Pb^{2+}	1000	97.4 ± 2.9
Cd^{2+}	1000	96.9 ± 1.6
Mg^{2+}	10,000	95.1 ± 2.5
Ca^{2+}	10,000	97.1 ± 3.5
Zn^{2+}	10,000	95.4 ± 2.3
Cu^{2+}	10,000	96.1 ± 2.7
Na^{+}	10,000	98.6 ± 2.1
Fe^{3+}	10,000	99.1 ± 3.5
Ag^{+}	10,000	97.6 ± 2.1
Cl^{-}	10,000	100.8 ± 2.2
NO_3^{-}	10,000	99.8 ± 2.9
SO_4^{2-}	10,000	98.3 ± 3.7
PO_4^{3-}	10,000	98.7 ± 4.0
CO_3^{2-}	10,000	98.8 ± 2.2

of 5 min; (d) 2 mL of mixture of 0.5 M HNO_3 and 2% thiourea as eluent solution; (e) volume of sample solution of 100 mL.

Interference studies

The effect of some common ions on the adsorption efficiency of Hg^{+2} was studied under the optimized conditions. In these experiments different concentrations of some possible interfering ions were added to 100 mL of standard solution containing 1 μg of Hg^{2+}. The results are summarized in Table 1. These data proved that the complex matrices such as seawater cannot affect the recovery of mercury ions adsorption. Furthermore, based on the performed examinations, the completion adsorption for mercury ion was obtained by 1000 μg L^{-1} of target analyte. Although, the trace level determination of mercury ions was aimed for the present work, the sorbent can completely adsorb mercury ions by mg L^{-1} levels.

Table 3 Determination of mercury ions in real water samples

Sample	Added (ng L^{-1})	Founded (ng L^{-1})	Recovery (%)
River water	0	N.D.[a]	–
	500	490.6	98.1 ± 2
	5000	5023.5	100.5 ± 3
Seawater	0	N.D.	–
	500	486.1	97.2 ± 3
	5000	4942.4	98.8 ± 3

[a] Not detected

Analytical figures of merit

The analytical methodology was investigated by reporting linearity, detection limit and preconcentration factor (PF) of the prepared sorbent for mercury determination. Under the experimental optimal conditions (pH: 6, amount of sorbent: 15 mg, sample volume: 100 mL, eluent volume: 2 mL), nine Hg^{2+} standard solutions were enriched and the eluting solutions were analyzed by CV-AAS. The results indicated that calibration curve was linear in the range of 0.1–40 μg L^{-1} with correlation coefficient (r) of 0.996. The limit of detection (LOD) of the method was studied under optimal conditions after application of the extraction procedure to the blank solutions. The LOD, calculated from $C_{LOD} = 3\ S_d/m$ (where C_{LOD}, S_d and m are the limit of detection, standard deviation of the blank and slope of a calibration curve, respectively), was 0.028 μg L^{-1}. The PF was calculated by the ratio of slopes of the calibration curves before and after preconcentration [29]. According to the result, the PF value was 49.

Table 2 compares the figures of merit of the present adsorbent with the other solid phases used in the literatures for extraction of mercury ion from different samples. It can be seen that some values of the suggested sorbent is more or less comparable with those of the other methods which are modified with various functional groups. However, the present sorbent is based on an

Table 2 Comparison of the method with other reported extraction techniques for determination of mercury

Extraction process	Analysis method	Detection limit (μg L^{-1})	Linear range (μg L^{-1})	Preconcentration factor	Ref.
Fe_3O_4@SnO_2 yolk-shell	CV-AAS	0.028	0.1–40	49	This work
GO–MC-MPTS[a]	CV-AAS	0.06	0.12–80	80	[30]
Ionic liquid based-preconcentration	CV-AAS	0.0023	0.01–2.5	36	[31]
SH@SiO_2/metal-organic framework nanocomposite	CV-AAS	0.02	0.1–80	167	[32]
Agar powder modified by 2-mercaptobenzimidazole	CV-AAS	0.02	0.04–2.4	13	[33]
Functionalized silica gel-SPE	CV-ETAAS	0.006	0.009–1.5	42	[34]
CPE-Hg-PONPE 7.5	ETAAS	0.00001	-	22	[35]

[a] Graphene oxide–magnetic chitosan grafted with 3-mercaptopropyltrimethoxysilane

inorganic substrate without any modification with functional groups. In this way, the prepared magnetic sorbent also introduces a low-cost adsorbent with fast kinetic of adsorption that is synthesized with green solvents.

Analysis of natural water samples

The validation and reliability of the introduced preconcentration procedure was examined by the analysis of two different natural water samples (Haraz River water and Seawater of Persian Gulf). The physicochemical characteristics of seawater sample were as following: pH: 8.4, dissolved O_2: 4.8 mg L^{-1}, conductivity: 57.7 ms cm^{-1} and total dissolved solid: 28.9 mg L^{-1}. The mercury was not detected in the real samples. To demonstrate the accuracy, water samples spiked with Hg^{2+} at two concentration levels of 0.5 μg L^{-1} and 5 μg L^{-1}. The data, listed in Table 3, shows that the recovery of Hg^{2+} was obtained over 97.2%. Based on U.S. Environmental Protection Agency (EPA) [30], the maximum allowable level of mercury in seawater can be 1.8 μg L^{-1} and performance data of the present method has provided the quantitative analyses lower than the mentioned concentration level. Accordingly, it clearly demonstrates that recoveries are satisfactory and the presented method is qualified to determine mercury ions according to the guideline level of EPA.

Conclusions

In summary, we have demonstrated an efficient rattle-type sorbent with a new synthetic methodology for solid phase extraction of trace amount of mercury. The SnO_2-shelled magnetic core with novel properties and without any modification indicated a high-performance for the preconcentration of Hg^{2+}. In fact, an inorganic substrate including of interstitial void is employed for adsorption of target analyte. Due to the presence of void, higher specific surface area is acquired which can cause more efficiency for a sorbent. The facile synthesis with green solvents, fast adsorption with satisfactory preconcentration factor and high accuracy are obtained for the present sorbent. The results proved this fact that the introduced sorbent has sufficient potential in extraction procedure and also the magnetic SnO_2 nanorattles can be attractive candidate materials for solid phase extraction of heavy metal ions. The relative low reusability and also low selectivity respect to analogous ions can be mentioned as the limitation of the introduced sorbent.

Acknowledgments We gratefully acknowledge the financial support for this work by the Iranian National Science Foundation with grant number of 94810824.

Compliance with ethical standards The author(s) declare that they have no competing interests.

References

1. Zeng T, Zhang X, Ma Y, Wang S, Niu H, Cai Y (2013) A functional rattle-type microsphere with a magnetic-carbon double-layered shell for enhanced extraction of organic targets. Chem Commun 49:6039–6041
2. Mahmoud ME, Ahmed SB, Osman MM, Abdel-Fattah TM (2015) A novel composite of nanomagnetite-immobilized-baker's yeast on the surface of activated carbon for magnetic solid phase extraction of Hg (II). Fuel 139:614–621
3. Liu J, Cheng J, Che R, Xu J, Liu M, Liu Z (2012) Double-shelled yolk–shell microspheres with Fe_3O_4 cores and SnO_2 double shells as high-performance microwave absorbers. The. J Phys Chem C 117:489–495
4. Han J, Chen R, Wang M, Lu S, Guo R (2013) Core–shell to yolk–shell nanostructure transformation by a novel sacrificial template-free strategy. Chem Commun 49:11566–11568
5. Liu J, Qiao SZ, Budi Hartono S, Lu GQM (2010) Monodisperse yolk–shell nanoparticles with a hierarchical porous structure for delivery vehicles and nanoreactors. Angew Chem 122:5101–5105
6. Liu J, Xu J, Che R, Chen H, Liu Z, Xia F (2012) Hierarchical magnetic yolk–shell microspheres with mixed barium silicate and barium titanium oxide shells for microwave absorption enhancement. J Mater Chem 22:9277–9284
7. Yang Y, Liu J, Li X, Liu X, Yang Q (2011) Organosilane-assisted transformation from core–shell to yolk–shell nanocomposites. Chem Mater 23:3676–3684
8. Priebe M, Fromm KM (2015) Nanorattles or yolk–Shell nanoparticles—what are they, how are they made, and what are they good for? Chem Eur J 21:3854–3874
9. Wang S, Zhang M, Zhang W (2011) Yolk − Shell catalyst of single Au nanoparticle encapsulated within hollow mesoporous silica microspheres. ACS Catal 1:207–211
10. Zhang L, Wang T, Li L, Wang C, Su Z, Li J (2012) Multifunctional fluorescent-magnetic polyethyleneimine functionalized Fe_3O_4–mesoporous silica yolk–shell nanocapsules for siRNA delivery. Chem Commun 48:8706–8708
11. Liu N, Wu H, McDowell MT, Yao Y, Wang C, Cui Y (2012) A yolk-shell design for stabilized and scalable Li-ion battery alloy anodes. Nano Lett 12:3315–3321
12. Liu J, Xia H, Xue D, Lu L (2009) Double-shelled nanocapsules of V_2O_5-based composites as high-performance anode and cathode materials for Li ion batteries. J Am Chem Soc 131:12086–12087
13. Roca M, Haes AJ (2008) Silica − Void − Gold nanoparticles: temporally stable surface-enhanced Raman scattering substrates. J Am Chem Soc 130:14273–14279
14. Ikeda S, Ishino S, Harada T, Okamoto N, Sakata T, Mori H, Kuwabata S, Torimoto T, Matsumura M (2006) Ligand-free platinum nanoparticles encapsulated in a hollow porous carbon Shell as a highly active heterogeneous hydrogenation catalyst. Angew Chem 118:7221–7224
15. Gao J, Liang G, Cheung JS, Pan Y, Kuang Y, Zhao F, Zhang B, Zhang X, Wu EX, Xu B (2008) Multifunctional yolk − shell nanoparticles: a potential MRI contrast and anticancer agent. J Am Chem Soc 130:11828–11833
16. Li G, Tang Z (2014) Noble metal nanoparticle@ metal oxide core/yolk–shell nanostructures as catalysts: recent progress and perspective. Nanoscale 6:3995–4011
17. Pan S, Li J, Wan G, Liu C, Fan W, Wang L (2016) Nanosized yolk–shell Fe_3O_4@Zr(OH)x spheres for efficient removal of Pb(II) from aqueous solution. J Hazard Mater 309:1–9
18. Liu Y, Jiao Y, Zhang Z, Qu F, Umar A, Wu X (2014) Hierarchical SnO_2 nanostructures made of intermingled ultrathin nanosheets for environmental remediation, smart gas sensor, and supercapacitor applications. ACS Appl Mater Interfaces 6:2174–2184
19. Liu T, Xue L, Guo X, Zheng CG (2014) DFT study of mercury adsorption on α-Fe_2O_3 surface: role of oxygen. Fuel 115:179–185

20. Zhang L, Huang T, Liu X, Zhang M, Li K (2011) Selective solid-phase extraction of trace thallium with nano-Al_2O_3 from environmental samples. J Anal Chem 66:368–372
21. JS H, Zhong LS, Song WG, Wan LJ (2008) Synthesis of hierarchically structured metal oxides and their application in heavy metal ion removal. Adv Mater 20:2977–2982
22. Rajabi HR, Shamsipur M, Zahedi MM, Roushani M (2015) On-line flow injection solid phase extraction using imprinted polymeric nanobeads for the preconcentration and determination of mercury ions. Chem Eng J 259:330–337
23. Adlnasab L, Ebrahimzadeh H, Asgharinezhad AA, Aghdam MN, Dehghani A, Esmaeilpour S (2014) A preconcentration procedure for determination of ultra-trace mercury (II) in environmental samples employing continuous-flow cold vapor atomic absorption spectrometry. Food Anal Methods 7:616–628
24. Ali TA, Mohamed GG (2015) Multi-walled carbon nanotube and nanosilica chemically modified carbon paste electrodes for the determination of mercury (ii) in polluted water samples. Anal Methods 7:6280–6289
25. Mehdinia A, Kayyal TB, Jabbari A, Aziz-Zanjani MO, Ziaei E (2013) Magnetic molecularly imprinted nanoparticles based on grafting polymerization for selective detection of 4-nitrophenol in aqueous samples. J Chromatography A 1283:82–88
26. Purbia R, Paria S (2015) Yolk/Shell nanoparticles: classifications, synthesis, properties, and applications. Nanoscale 7:19789–19873
27. Liu J, Cheng J, Che R, Xu J, Liu M, Liu Z (2013) Synthesis and microwave absorption properties of yolk–shell microspheres with magnetic iron oxide cores and hierarchical copper silicate shells. ACS Appl Mater Interfaces 5:2503–2509
28. Zhang X, Ren H, Wang T, Zhang L, Li L, Wang C, Su Z (2012) Controlled synthesis and magnetically separable photocatalytic properties of magnetic iron oxides@SnO_2 yolk–shell nanocapsules. J Mater Chem 22:13380–13385
29. Mehdinia A, Khodaee N, Jabbari A (2015) Fabrication of graphene/Fe_3O_4@ polythiophene nanocomposite and its application in the magnetic solid-phase extraction of polycyclic aromatic hydrocarbons from environmental water samples. Anal Chim Acta 868:1–9
30. Ziaei E, Mehdinia A, Jabbari A (2014) A novel hierarchical nanobiocomposite of graphene oxide–magnetic chitosan grafted with mercapto as a solid phase extraction sorbent for the determination of mercury ions in environmental water samples. Anal Chim Acta 850:49–56
31. Martinis EM, Bertón P, Olsina RA, Altamirano JC, Wuilloud RG (2009) Trace mercury determination in drinking and natural water samples by room temperature ionic liquid based-preconcentration and flow injection-cold vapor atomic absorption spectrometry. J Hazard Mater 167:475–481
32. Sohrabi MR (2014) Preconcentration of mercury(II) using a thiol-functionalized metal-organic framework nanocomposite as a sorbent. Microchim Acta 181:435–444
33. Pourreza N, Ghanemi K (2009) Determination of mercury in water and fish samples by cold vapor atomic absorption spectrometry after solid phase extraction on agar modified with 2-mercaptobenzimidazole. J Hazard Mater 161:982–987
34. Alonso EV, Cordero MS, de Torres AG, Rudner PC, Pavón JC (2008) Mercury speciation in sea food by flow injection cold vapor atomic absorption spectrometry using selective solid phase extraction. Talanta 77:53–59
35. Aranda PR, Gil RA, Moyano S, De Vito IE, Martinez LD (2008) Cloud point extraction of mercury with PONPE 7.5 prior to its determination in biological samples by ETAAS. Talanta 75:307–311